

Electronic Supplementary Information (ESI)

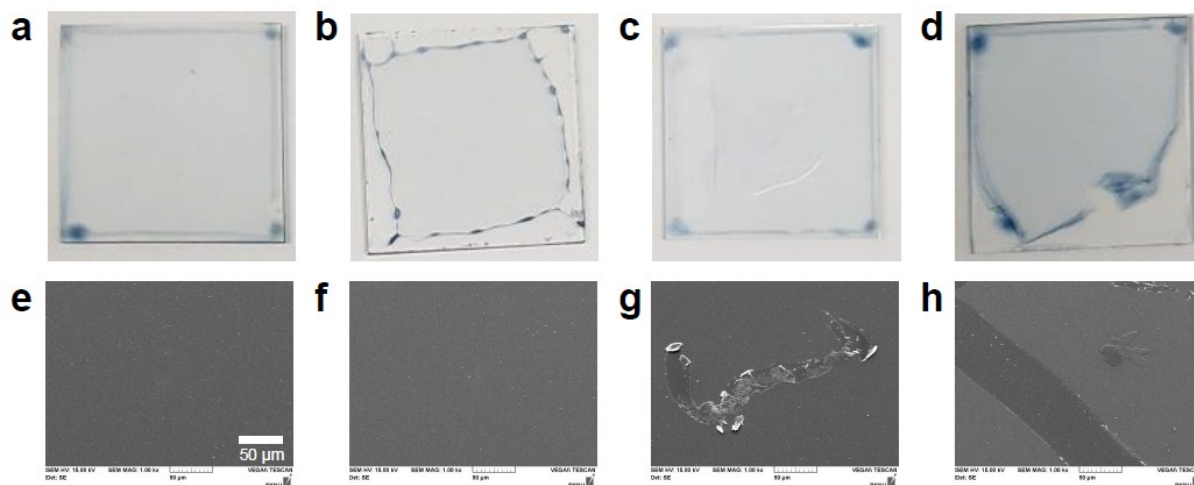


Figure S1. Coating properties of PEDOT:PSS films. Photographs and SEM images of (a, e) the laser-treated PEDOT:PSS film ($\sigma \sim 700 \text{ S cm}^{-1}$), (b, f) the EG (6 vol. %)-mixed PEDOT:PSS film ($\sigma \sim 700 \text{ S cm}^{-1}$), (c, g) the methanol post-treated PEDOT:PSS film ($\sigma \sim 1300 \text{ S cm}^{-1}$), and (d, h) the H_2SO_4 post-treated PEDOT:PSS film ($\sigma \sim 2300 \text{ S cm}^{-1}$). These films were spin-coated on glass substrates. All substrates were treated with oxygen plasma for more than 10 min. The EG-mixed PEDOT:PSS film exhibits poor wetting properties on the glass substrate. Post-treated films show peeling-off the PEDOT:PSS films from the supporting glass substrates and residues on the surface of films.

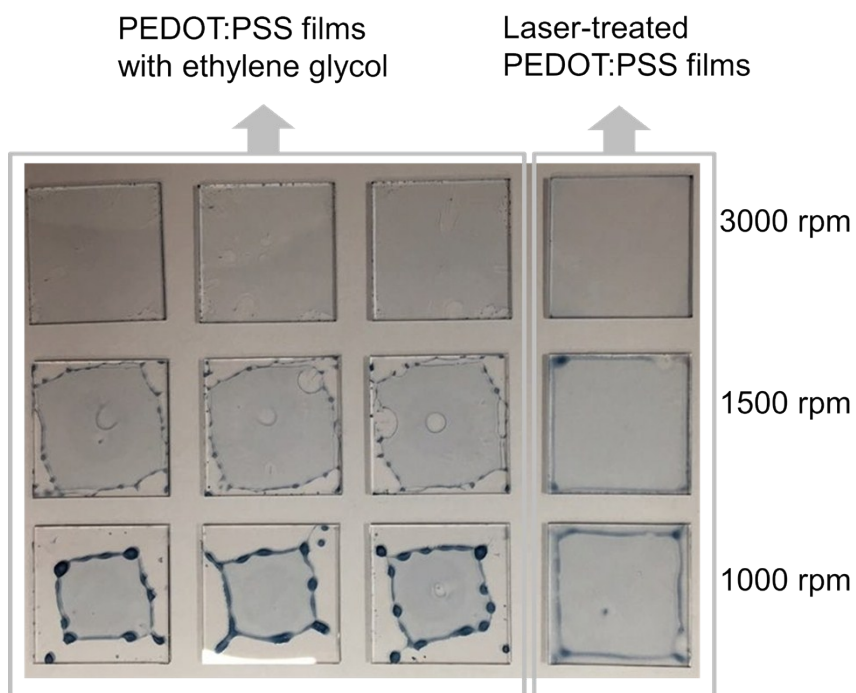
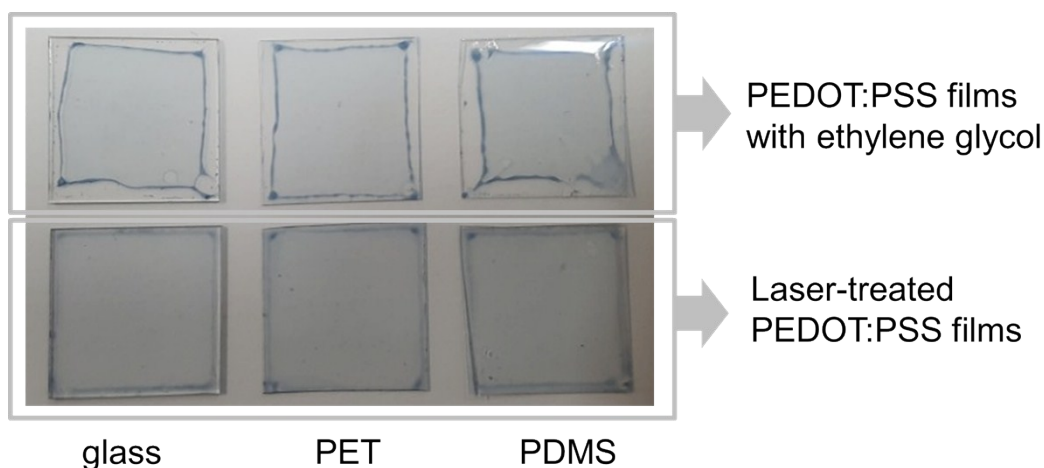
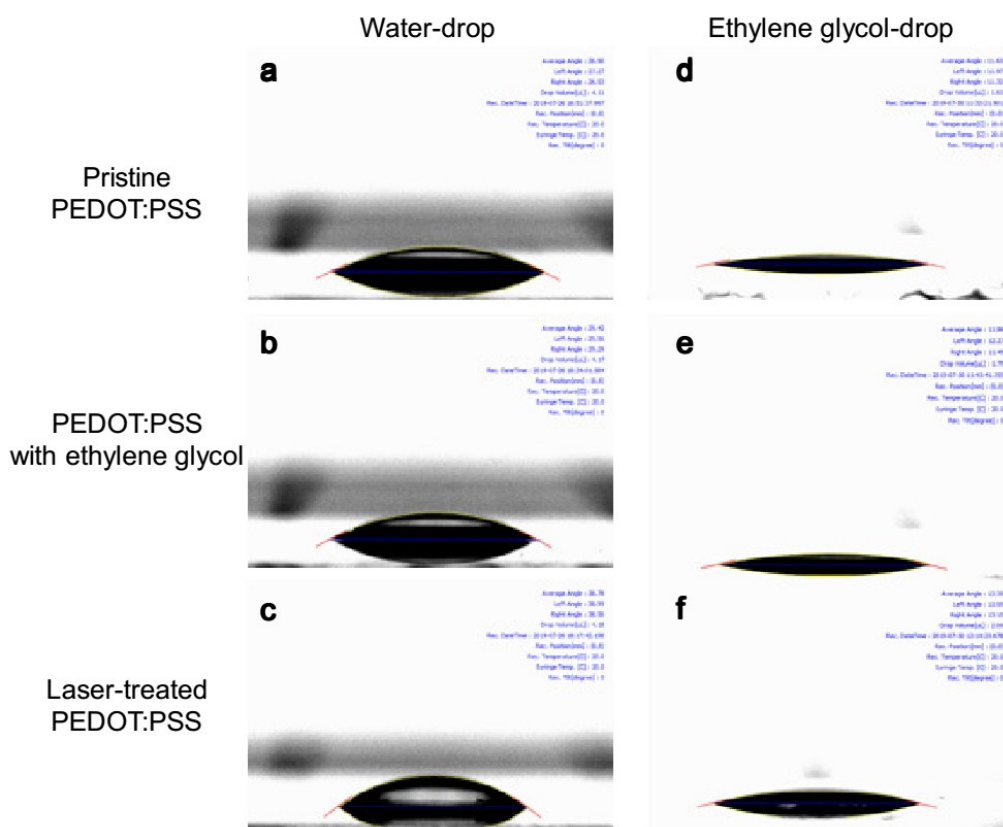


Figure S2. Photographs for EG (6 vol .%)-doped and laser-treated PEDOT:PSS films on glass substrates. All substrates were treated with oxygen plasma for more than 10 min. The EG-doped PEDOT:PSS films show poor wetting properties due to a high viscosity of solutions. In contrast, laser-treated PEDOT:PSS films show the excellent film formation.



| | glass | PET | PDMS |
|--------------------------------|------------------------------------|------------------------------------|------------------------------------|
| PEDTO:PSS with ethylene glycol | 210 (7) Ω sq ⁻¹ | 219 (25) Ω sq ⁻¹ | not measurable |
| Laser-treated PEDOT:PSS | 159 (11) Ω sq ⁻¹ | 175 (16) Ω sq ⁻¹ | 178 (18) Ω sq ⁻¹ |

Figure S3. Photographs for EG (6 vol .%) -doped and laser-treated PEDOT:PSS films on various substrates such as glass, PET, and PDMS. All substrates were treated with oxygen plasma for more than 10 min. The EG-doped PEDOT:PSS films show poor wetting properties due to a high viscosity of solutions. In contrast, laser-treated PEDOT:PSS films show the excellent film formation on the various substrates. The numbers in the parenthesis indicate the standard deviation of sheet resistance.



| | Surface energy | Polar fraction | Non-Polar fraction |
|--------------------------------|----------------------------|----------------------------|---------------------------|
| Pristine PEDOT:PSS | 75.5 dyne cm ⁻¹ | 71.6 dyne cm ⁻¹ | 3.9 dyne cm ⁻¹ |
| PEDTO:PSS with Ethylene glycol | 69.8 dyne cm ⁻¹ | 64.3 dyne cm ⁻¹ | 5.4 dyne cm ⁻¹ |
| Laser-treated PEDTO:PSS | 59.4 dyne cm ⁻¹ | 50.0 dyne cm ⁻¹ | 9.4 dyne cm ⁻¹ |

Figure S4. Droplet images of (a, d) pristine PEDOT:PSS, (b, e) EG-mixed PEDOT:PSS, and (c, f) laser-treated PEDOT:PSS films. The contact angle measurements for various PEDOT:PSS films were carried out using water (left) and ethylene glycol (right). The laser-treated PEDOT:PSS film exhibits the larger water contact angle (38.7°) than the pristine and EG-mixed PEDOT:PSS films (24.0° and 29.3° , respectively) due to the decrease in surface energy. This result indicates that hydrophilic PSS on the surface of film is removed by laser treatment, which is consistent with the results of XPS and KPFM measurements that clearly show the reduction of the surface PSS. For the pristine, EG-mixed, and laser-treated PEDOT:PSS films, the obtained contact angles of ethylene glycol droplet were 11.6° , 11.8° , and 13.4° , respectively. The calculated surface energy is listed in the table.

The laser-treated PEDOT:PSS films exhibit the decrease in polar fraction and the increase in disperse (non-polar) fraction, which are attributed to the removal of surface PSS after laser treatment. Since most solution-processed OPV cells and OLEDs use non-polar solvent-based solutions for active layers, it is expected that the device performance and fabrication process are not considerably affected by the wetting performance of laser-treated PEDOT:PSS films. These are supported by the results of OPV cells with a conventional structure (PEDOT:PSS/active layer/LiF/Al) (Fig. S8, ESI[†]).

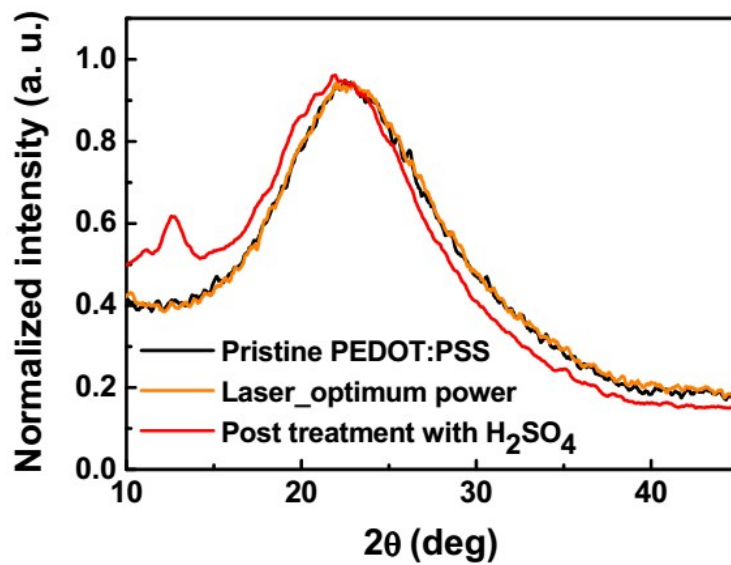


Figure S5. The X-ray diffraction (XRD) pattern of PEDOT:PSS films. The peak at $2\theta = 23^\circ$ corresponds to the (020) reflection of PEDOT, related to interchain planar ring stacking of PEDOT. The XRD result shows that both PEDOT:PSS films with and without laser treatment have the similar crystalline structures of PEDOT:PSS with a single peak at $2\theta = 23^\circ$.^[20, S1] In contrast, the H₂SO₄-treated PEDOT:PSS film exhibits the double-peak crystallography pattern due to the change of crystallinity and phase separations by H₂SO₄ treatment.

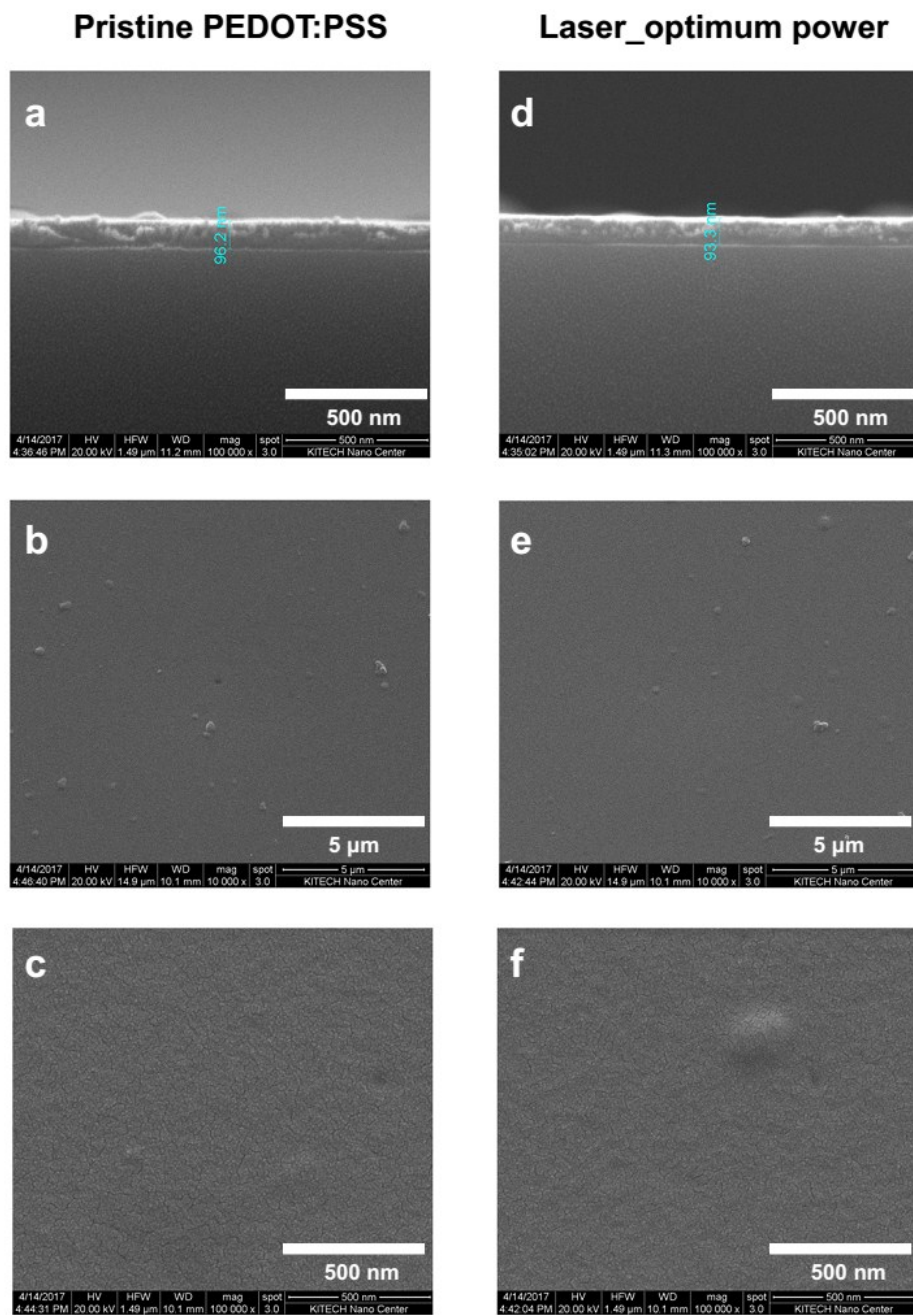


Figure S6. SEM images of PEDOT:PSS films. SEM images for (a, b, c) the pristine PEDOT:PSS and (d, e, f) the laser-treated PEDOT:PSS film, showing similar surface characteristics.

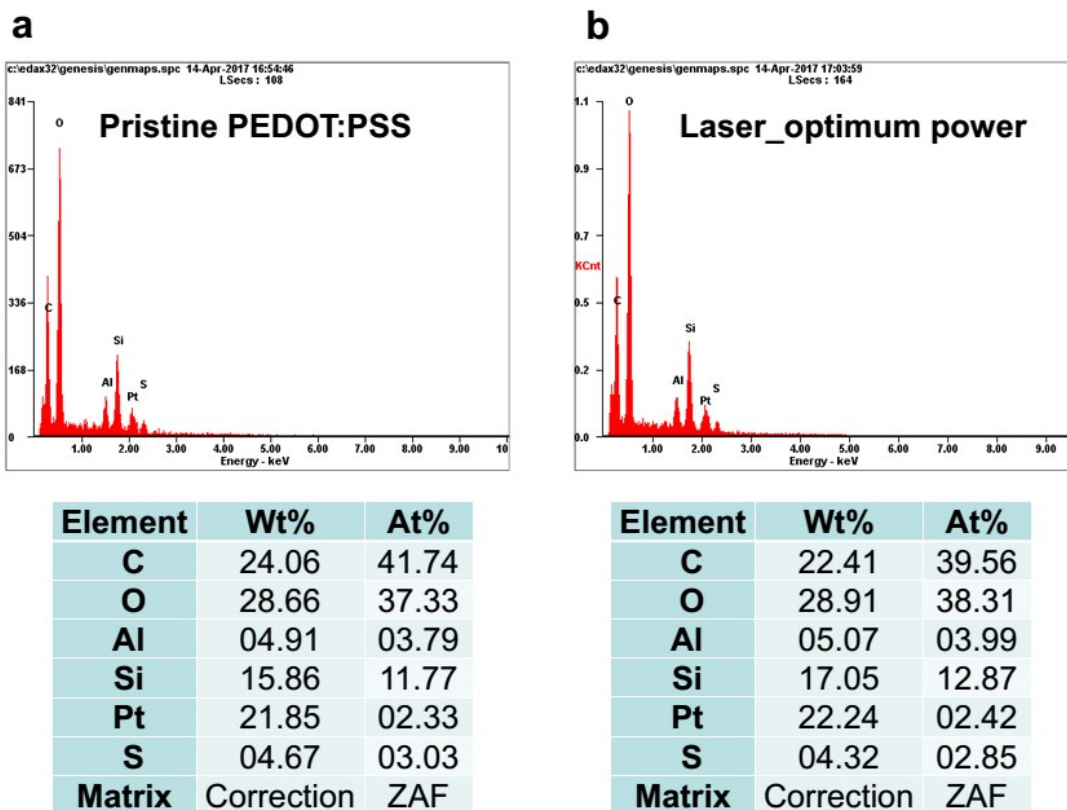


Figure S7. SEM-EDX analysis of (a) pristine PEDOT:PSS and (b) laser treated PEDOT:PSS films. The amount of carbon (C), oxygen (O) and sulfur (S) are almost conserved after laser-treatment.

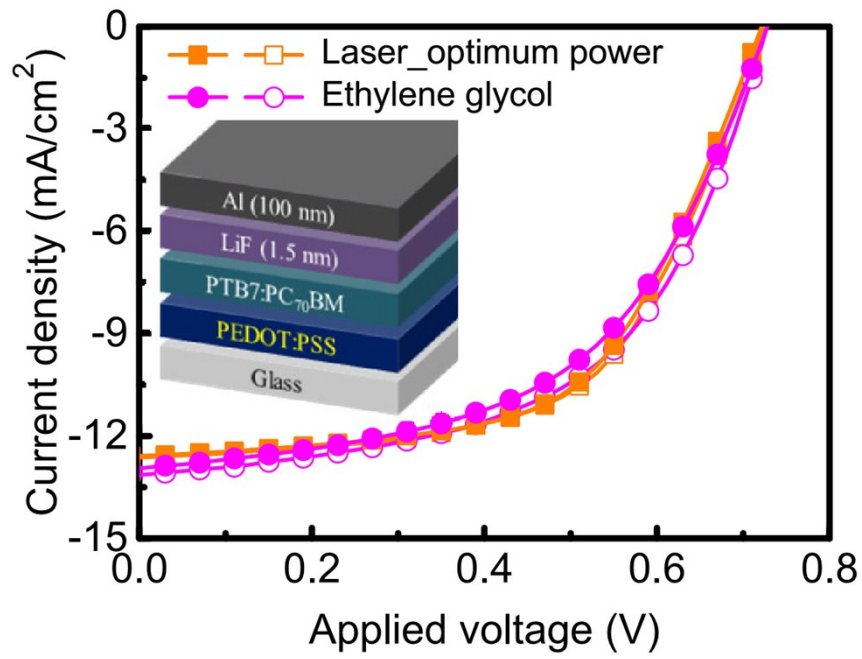


Figure S8. Current-density-voltage curves of OPV cells with the conventional structure based on the PEDOT:PSS films (filled symbols: $\sim 120 \text{ ohm sq}^{-1}$, open symbols: $\sim 90 \text{ ohm sq}^{-1}$).



Figure S9. Photograph of the laser system.

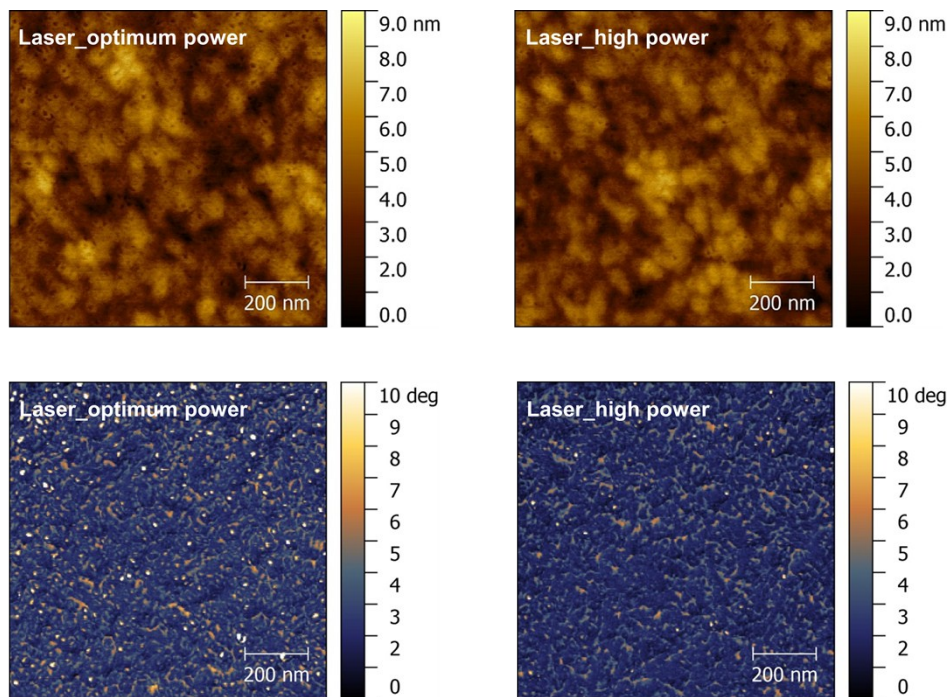


Figure S10. AFM topography (top) and phase images (bottom) for laser-treated PEDOT:PSS films with optimum and high laser power. The possible deformation of polymer structures by irradiating laser with high power is not observed in topographic and phase images.

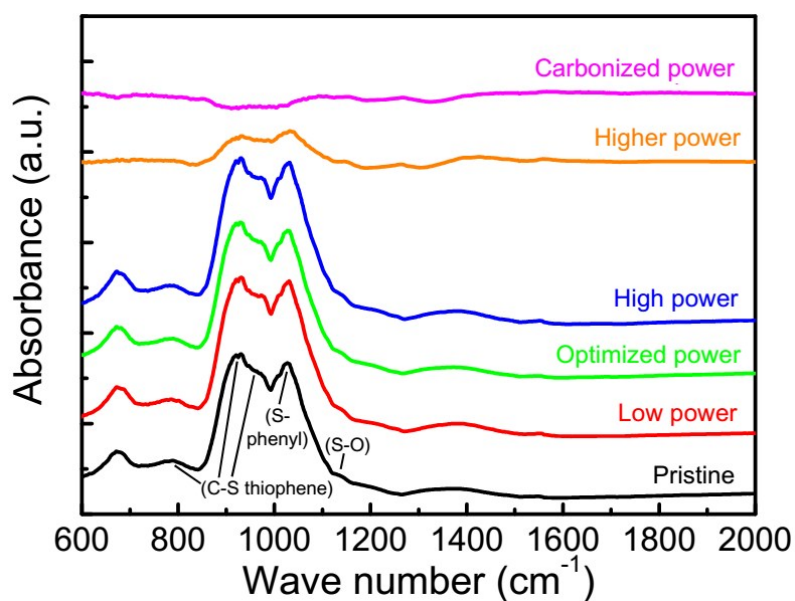


Figure S11. FTIR spectra of PEDOT:PSS films treated with various laser powers. The irradiation conditions for laser-treated PEDOT:PSS films were 0, 1.7, 2.3, 2.7, 2.8, and 2.9 W cm^{-2} for pristine, low-power, optimized-power, high-power, higher-power, and carbonized power samples, respectively. The bands from 800 to 1100 cm^{-1} are mainly associated with PEDOT structures and the bands above 1100 cm^{-1} are attributed to PSS-structures [S2, S3]. The PEDOT:PSS films irradiated with a laser power below the extreme condition (2.8 and 2.9 W cm^{-2}) did not exhibit a remarkable change of FTIR results. However, a partial damage, decomposition, or deformation of polymer structures are still certainly expected by considering the increase in sheet resistance at the high laser power (2.7 W cm^{-2}). The FTIR measurements were performed by Spotlight 400, PerkinElmer.

Table S1. The characteristics of the laser-treated PEDOT:PSS films. Thicknesses, sheet resistances, and conductivities for laser-treated PEDOT:PSS films with optimum laser power as a function of spin-speed.

| | | | | | | | |
|----------|--------------------------------------|-------|-------|-------|-------|-------|-------|
| 1000 rpm | thickness (nm) | 118.0 | 122.4 | 119.5 | | | |
| | sheet R ($\Omega \text{ sq}^{-1}$) | 113.5 | 96.2 | 108.2 | | | |
| | conductivity (S cm^{-1}) | 746.7 | 849.7 | 773.3 | | | |
| 1500 rpm | thickness (nm) | 93.3 | 93.3 | 97.6 | 99.1 | 97.6 | 96.2 |
| | sheet R ($\Omega \text{ sq}^{-1}$) | 151.7 | 151.4 | 136.1 | 112.5 | 134.6 | 150.6 |
| | conductivity (S cm^{-1}) | 706.6 | 707.9 | 752.7 | 897.0 | 761.2 | 690.3 |
| 1800 rpm | thickness (nm) | 80.1 | 80.1 | 87.4 | 81.6 | | |
| | sheet R ($\Omega \text{ sq}^{-1}$) | 165.0 | 160.5 | 132.2 | 137.3 | | |
| | conductivity (S cm^{-1}) | 756.6 | 777.8 | 865.3 | 892.4 | | |
| 2000 rpm | thickness (nm) | 77.2 | 74.3 | 74.3 | | | |
| | sheet R ($\Omega \text{ sq}^{-1}$) | 139.0 | 161.7 | 169.8 | | | |
| | conductivity (S cm^{-1}) | 931.9 | 832.3 | 792.5 | | | |
| 2500 rpm | thickness (nm) | 65.6 | 67.0 | 69.9 | 67.0 | | |
| | sheet R ($\Omega \text{ sq}^{-1}$) | 216.8 | 203.7 | 162.9 | 203.5 | | |
| | conductivity (S cm^{-1}) | 703.1 | 732.7 | 878.2 | 733.4 | | |

Table S2. Sheet resistances of heated PEDOT:PSS films. Sheet resistances for pristine PEDOT:PSS films with respect to the temperature of hot plate, where PEDOT:PSS films on glass were kept for 10 min on hot plate with the corresponding temperature. The sheet resistances were measured after cooling down to room temperature. At a temperature of 330 °C, the color of PEDOT:PSS film changed to dark due to excessive heat and lost a conductivity.

| Temperature (°C) | Sheet resistance ($\Omega \text{ sq}^{-1}$) |
|------------------|---|
| - | 811403.5 |
| 150 | 624332.2 |
| 210 | 591631.3 |
| 270 | 286501.2 |
| 330 | - |

Table S3. Sheet resistances of laser-treated PEDOT:PSS films. Sheet resistances for PEDOT:PSS films as a function of irradiated laser power and spin-speed.

| 1000 rpm | | 1500 rpm | | 1800 rpm | | 2000 rpm | | 2500 rpm | |
|-----------|--------------------------------------|-----------|--------------------------------------|-----------|--------------------------------------|-----------|--------------------------------------|-----------|--------------------------------------|
| power (W) | sheet R ($\Omega \text{ sq}^{-1}$) | power (W) | sheet R ($\Omega \text{ sq}^{-1}$) | power (W) | sheet R ($\Omega \text{ sq}^{-1}$) | power (W) | sheet R ($\Omega \text{ sq}^{-1}$) | power (W) | sheet R ($\Omega \text{ sq}^{-1}$) |
| 0 | 62000 | 0 | 75600 | 0 | 82000 | 0 | 94100 | 0 | 113000 |
| 1.53 | 1058.2 | 1.04 | 5965.7 | 2.98 | 137.3 | 2.01 | 4374.3 | 3.57 | 400 |
| 1.72 | 588 | 2.56 | 140.4 | 3.18 | 214.1 | 2.4 | 1358.4 | 3.66 | 190 |
| 1.82 | 96.1 | 2.6 | 126.5 | 3.27 | 555.2 | 3.18 | 169.8 | 3.76 | 354 |
| 1.92 | 1092.1 | 2.69 | 225.9 | | | 3.27 | 161.7 | 3.95 | 1190 |
| | | | | | | 3.37 | 474.9 | | |
| | | | | | | 3.57 | 1179.7 | | |

Table S4. Sheet resistances of EG-doped PEDOT:PSS films with laser treatment. Sheet resistances for EG (6 vol.%) -doped PEDOT:PSS films (spin-speed: 1000 rpm) as a function of laser power after laser treatment. Due to thicker films, a lower laser power is applied.

| Laser power (W) | Sheet resistance ($\Omega \text{ sq}^{-1}$) |
|------------------------|---|
| - | 90.2 |
| 1 | 115.6 |
| 1.1 | 100.7 |
| 1.3 | 97.4 |
| 1.5 | 124.1 |
| 1.7 | 696.5 |

Table S5. Device parameters for solar cells with the conventional structure (PEDOT:PSS/active layer/LiF/Al).

| | R_{sh} ($\Omega \text{ sq}^{-1}$) | V_{OC} (V) | J_{SC} (mA cm^{-2}) | FF (%) | η (%) |
|--|---------------------------------------|-------------------|----------------------------------|----------------|------------------|
| OPV cells with laser-treated PEDOT:PSS | 90 | 0.721 | 12.58 | 58.5 | 5.312 |
| | 90 | 0.725 | 12.63 | 58.8 | 5.379 |
| | 90 | 0.725 | 12.52 | 58.7 | 5.328 |
| | average | 0.724 ± 0.002 | 12.57 ± 0.06 | 58.7 ± 0.1 | 5.340 ± 0.03 |
| OPV cells with EG-mixed PEDOT:PSS | 90 | 0.728 | 12.95 | 52.8 | 4.979 |
| | 90 | 0.728 | 13.13 | 54.9 | 5.246 |
| | 90 | 0.728 | 12.58 | 48.6 | 4.455 |
| | average | 0.728 ± 0.000 | 12.89 ± 3.21 | 52.1 ± 3.2 | 4.893 ± 0.40 |

Table S6. Device parameters for inverted solar cells (PEDOT:PSS/ZnO/active layer/MoO_x/Al).

| | R _{sh} ($\Omega \text{ sq}^{-1}$) | V _{OC} (V) | J _{SC} (mA cm ⁻²) | FF | η (%) |
|--|--|---------------------|--|------|------------|
| OPV cells with laser-treated PEDOT:PSS | 120 | 0.72 | 12.1 | 0.49 | 4.3 |
| | 90 | 0.73 | 13.5 | 0.50 | 5.0 |
| OPV cells with EG-mixed PEDOT:PSS | 120 | 0.71 | 13.2 | 0.44 | 4.1 |
| | 90 | 0.71 | 13.1 | 0.53 | 4.9 |

Supplementary references

- [1] Wang, Q., Ahmadian-Yazdi, M. R. & Eslamian, M. Investigation of morphology and physical properties of modified PEDOT: PSS films made via in-situ grafting method. *Synth. Met.* **209**, 521–527 (2015).
- [2] Sriprachuabwong, C., Karuwan, C., Wisitsorrat, A., Phokharatkul, D., Lomas, T., Sritongkham, P. & Tuantranont, A. Inkjet-printed graphene-PEDOT:PSS modified screen printed carbon electrode for biochemical sensing. *J. Mater. Chem.* **22**, 5478-5485 (2012)
- [3] Mukherjee, S., Singh, R., Gopinathan, S., Murugan, S., Gawali, S., Saha, B., Biswas, J., Lodha, S. & Kumar, A. Solution-Processed Poly(3,4-ethylenedioxythiophene) Thin Films as Transparent Conductors: Effect of p-Toluenesulfonic Acid in Dimethyl Sulfoxide. *ACS Appl. Mater. Interfaces* **6**, 17792-17803 (2014)